Development of an Empirical Model for the Wear Rate of Contact Bearing Materials Using a Standard Pin-On-Disc Test

Ahmad Abdullah Alhumaidah[1*], Hadyan Ali Alajmi[2]

[1]Mechanical Engineer, Vocational Training Institute, The Public Authority for Applied Education and Training, Temple University, Philadelphia, **USA**
[2]Specialist Trainer (G), Public Authority for Applied Education and Training, University of Arab Academy for Science, Technology and Transport, **KUWAIT**

[*]Corresponding Contact:
Email: aa.alhumaidah@paaet.edu.kw

ABSTRACT

The wear rate for contact bearing materials is studied as a function of a number of potentially influential factors, including applied load, rotational speed, sliding distance, and material type. A standard pin-on-disc test is used to conduct this study. Two levels of applied load (20 and 10 N), rotational speed (100 and 200 rpm), sliding distance (150 and 450 m), and material type (AISI 440C and AISI 420 martensitic stainless steel) were tested. Tests is run according to the design of experiments (DOE) methodology. Experimental results are analyzed based on the analysis of variance (ANOVA) approach in order to determine the factors that have a significant impact on the wear rate. An empirical model is developed to fit the true relationship between wear rate and the significant factors in the case AISI 440C and AISI 420 materials. Finally, the morphology of the worn surface is studied using SEM and EDX images.

12/29/2018	Source of Support: None, NoConflict of Interest: Declared

INTRODUCTION

Wear can generally lead to severe economic and technological problems as it is the effect on resource utilization, machine performance, national economy and conservation of fuel. Therefore, the control of wear becomes a very strong need to eliminate and reduce its effects by studying the factors influences in the wear (Andersson et al., 2011; Andersson, 2012).

Wear is a surface phenomenon that depends on material properties such as hardness (Berglund and Shi, 2017), microstructure (Blau, 2015) and surface finish, and working conditions such as load, speed, lubrication, and temperature. Different conditions can cause

wear by different mechanisms. Generally, small changes in speed, load or environmental conditions can typically lead to considerable changes in the material wear rate of two or one surfaces in contact (Boher, 2009; Cavalieri et al., 2016).

A common way, which is used in order to measure wear rate is a pin-on-disc test based on the ASTM G99 standard. The test material is usually made in the form of a pin (Chongyi et al., 2013). This pin is setup to apply a certain force against a rotating disc at a constant rotational speed (w). Mass loss due to wear is then measured after some period of time. The wear rate (mm3/N.m) is then calculated according to the equation (Wang et al., 1996)

$$\text{Wear Rate} = \frac{M}{\rho F L} \qquad (1)$$

Where that M represents the mass loss (g), F refers to the applied load against the pin (N), the alloy density of the test specimens (g/mm3) represented by ρ, as well as L represents the length of distance of the sliding (m).

The previous equation can be useful for comparing between materials in terms of their wear resistance. However, this comparison may be accurate or reliable when the wear rate is measured at the same conditions of applied load, rotational speed, run length and surface finish. But when such conditions are different, the above equation is known to give different results. Thus, it will be very advantageous for practical reasons to have an empirical model for wear rate that is less sensitive to the various levels of process conditions.

AIMS AND OBJECTIVES

This paper aims to develop an Empirical Model for the Wear Rate of Contact Bearing Materials Using a Standard Pin-On-Disc Test, three main objectives are set to reach paper aim:

- Determine the sensitivity of the wear rate against the relevant process conditions for two commonly used contact bearing materials: AISI 440C and AISI 420 martensitic stainless steel.
- Develop an empirical relationship between wear rate and all the significant factors.
- Determine the morphology of the worn surface of the studied materials

METHODOLOGY

This part includes a description of AISI 440C and AISI 420 Martensitic stainless steel, the generation the DOE design, material preparation, the dry sliding wear tests and examination of surface morphology. Figure 1 shows a flow chart of the paper procedures and tests.

Material description
Samples Preparations
Design the experiment
Dry Sliding Wear tests
Examination of Surface Morphology
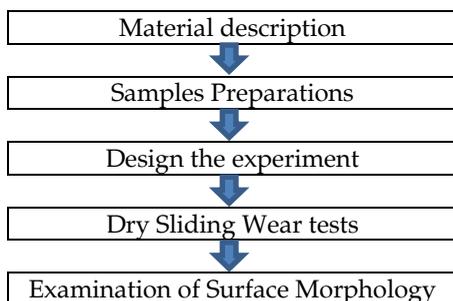
Figure 1: Paper methodology

RESULTS AND DISCUSSION

Table 1 shows experimental results of the dry sliding wear that are obtained through pin-on-disc tests. This table shows two levels for each factor with center points. The data are listed based on their random run order, which are produced through using Minitab software. Further, the process parameters impact on the wear weight loss has been investigated through (ANOVA) test.

Table 1: Experimental results of the dry sliding wear experiments

Run Order	Load (N)	Speed (rpm)	Distance (m)	Material Type	Mass Loss	Run Order	Load (N)	Speed (rpm)	Material Type	Distance (m)	Mass Loss
1	20	100	200	AISI 440C	0.0109	21	20	100	AISI 440C	200	0.0105
2	10	200	600	AISI 420HC	0.0138	22	20	200	AISI 440C	600	0.0151
3	20	100	200	AISI 420HC	0.0075	23	15	150	AISI 440C	400	0.0148
4	10	100	200	AISI 440C	0.0061	24	10	200	AISI 420HC	200	0.0043
5	10	200	600	AISI 420HC	0.0140	25	20	100	AISI 420HC	200	0.0073
6	10	100	600	AISI 420HC	0.0246	26	15	150	AISI 420HC	400	0.0149
7	20	100	600	AISI 440C	0.0274	27	10	200	AISI 420HC	200	0.0054
8	10	200	600	AISI 440C	0.0160	28	15	150	AISI 440C	400	0.0094
9	10	100	200	AISI 420HC	0.0054	29	20	100	AISI 420HC	600	0.0231
10	20	200	200	AISI 420HC	0.0051	30	10	100	AISI 440C	600	0.0226
11	20	200	600	AISI 420HC	0.0120	31	10	200	AISI 440C	600	0.0140
12	10	200	200	AISI 440C	0.0071	32	20	200	AISI 440C	600	0.0129
13	10	100	600	AISI 440C	0.0217	33	15	150	AISI 440C	400	0.0104
14	15	150	400	AISI 420HC	0.0124	34	10	200	AISI 440C	200	0.0048
15	20	200	200	AISI 440C	0.0077	35	15	150	AISI 420HC	400	0.0108
16	10	100	600	AISI 420HC	0.0238	36	10	100	AISI 420HC	200	0.0042
17	15	150	400	AISI 440C	0.0127	37	20	200	AISI 420HC	200	0.0057
18	20	200	600	AISI 420HC	0.0154	38	10	100	AISI 440C	200	0.0050
19	20	100	600	AISI 420HC	0.0223	39	15	150	AISI 420HC	400	0.0115
20	20	200	200	AISI 440C	0.0057	40	20	100	AISI 440C	600	0.0213

Analysis of Variance (ANOVA)

The ANOVA is applied on the model by using 95% a confidence level. The obtained results of ANOVA analyses for weight loss are shown in Table 2. It can be noted from the table that the P-value for the sliding speed, length of sliding distance and their interaction is lower than 0.05 which imply that both factors and their interaction have a significant effect on the weight loss at the confidence level 95%. On the other hand, the P-value of the applied load and materials factors is more than 0.05, which mean that these factors are not significant and they are not influenced on the weight loss. Moreover, the result in Table 1 shows that the length of sliding distance factor is the most significant and its contribution is 72.28% followed by sliding speed and the length-speed interaction that having 13.32% and 7.25% contribution respectively.

Table 2: ANOVA for the dry sliding wear rate

Source	DF	Seq SS	Contribution	Adj SS	Adj MS	F-Value	P-Value
Model	16	0.001616	95.99%	0.001616	0.000101	34.41	0.000
Linear	4	0.001454	86.37%	0.001454	0.000363	123.84	0.000
Load	1	0.000009	0.54%	0.000009	0.000009	3.11	0.091
Speed	1	0.000224	13.32%	0.000224	0.000224	76.39	0.000
Length	1	0.001216	72.28%	0.001216	0.001216	414.49	0.000
Material	1	0.000004	0.24%	0.000004	0.000004	1.35	0.257
2-Way Interactions	6	0.000150	8.91%	0.000150	0.000025	8.51	0.000
Load*Speed	1	0.000009	0.52%	0.000009	0.000009	2.97	0.098
Load*Length	1	0.000011	0.68%	0.000011	0.000011	3.88	0.061
Load*Material	1	0.000004	0.24%	0.000004	0.000004	1.36	0.256
Speed*Length	1	0.000122	7.25%	0.000122	0.000122	41.59	0.000
Speed*Material	1	0.000000	0.00%	0.000000	0.000000	0.00	0.976
Length*Material	1	0.000004	0.22%	0.000004	0.000004	1.27	0.272
3-Way Interactions	4	0.000010	0.59%	0.000010	0.000002	0.85	0.510
Load*Speed*Length	1	0.000003	0.15%	0.000003	0.000003	0.88	0.357
Load*Speed*Material	1	0.000006	0.35%	0.000006	0.000006	2.00	0.171
Load*Length*Material	1	0.000000	0.00%	0.000000	0.000000	0.00	0.976
Speed*Length*Material	1	0.000001	0.09%	0.000001	0.000001	0.51	0.484
4-Way Interactions	1	0.000001	0.03%	0.000001	0.000001	0.20	0.661
Load*Speed*Length*Material	1	0.000001	0.03%	0.000001	0.000001	0.20	0.661
Curvature	1	0.000001	0.08%	0.000001	0.000001	0.49	0.493
Error	23	0.000068	4.01%	0.000068	0.000003		
Lack-of-Fit	1	0.000004	0.22%	0.000004	0.000004	1.25	0.276
Pure Error	22	0.000064	3.79%	0.000064	0.000003		
Total	39	0.001683	100.00%				

The normal plot of the standardized effects in Figure 2 shows that the length (represented by C symbol) is significant and had a positive effect on the weight loss. Sliding speed and length/speed interaction (represented by B and BC symbols) are significant and have a negative effect in the mass loss.
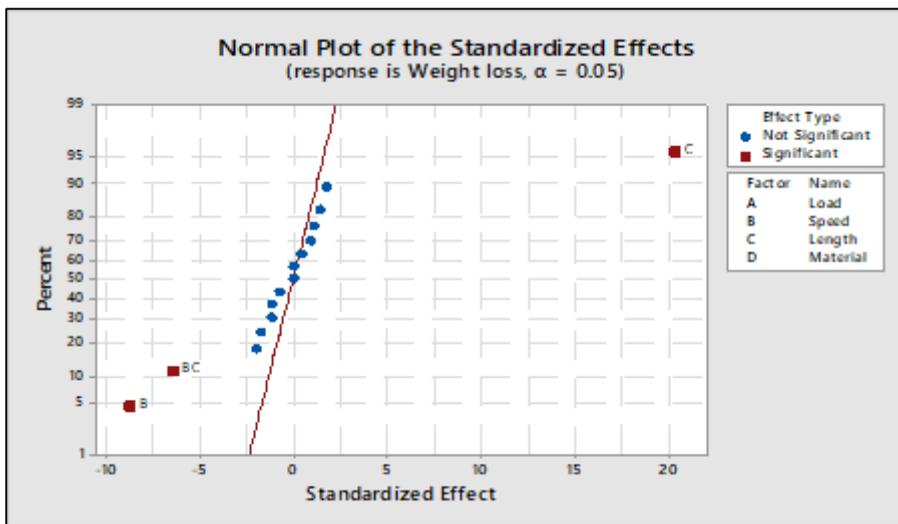
Figure 2: Normal curve for the standardized effect of the weight loss

Figure 3 shows the Pareto chart of the standardized effect. The chart shows the importance and the magnitude of the effects. The bars cross the red line (length, speed, and their interaction bars) at 2.07 are significant.
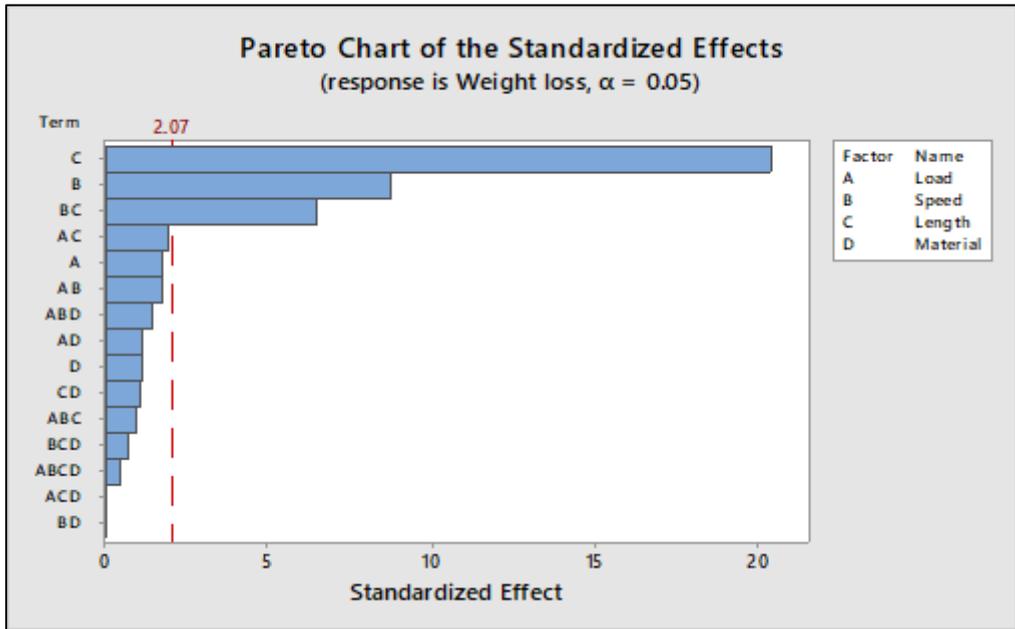
Figure 3: Pareto chart of the weight loss factors

The significance of the weight loss factors can be checked also by analyzing their main-effect-plots as illustrated in Figure 4. So, it can be noticed from the plot that both normal load and material had a very small effect on the weight loss, but the length and sliding speed had a high effect on the weight loss. Furthermore, the increase in length leads to increase the mass loss, but the increase in sliding speed leads to reduce the mass loss.
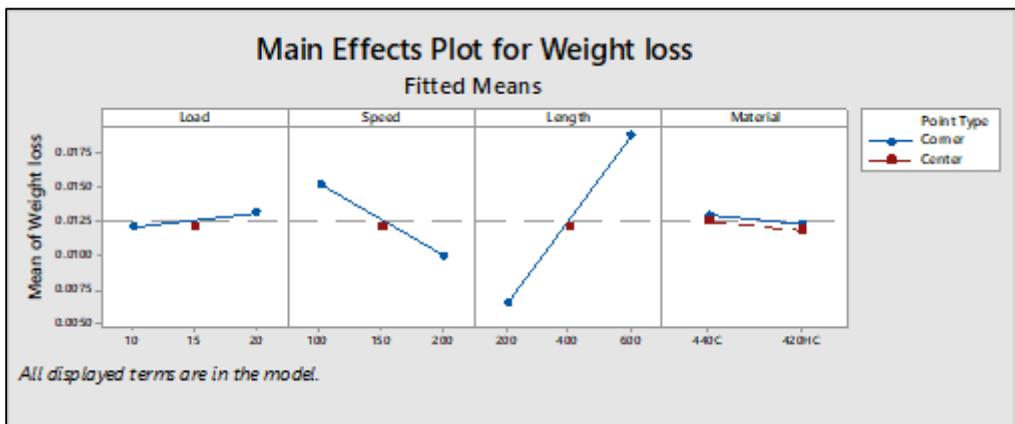
Figure 4: Effect of weight loss

Figure 5 shows the interaction plot for the weight loss. It can be noticed from the plots that the mass loss at the high speed and low length had a significant effect.
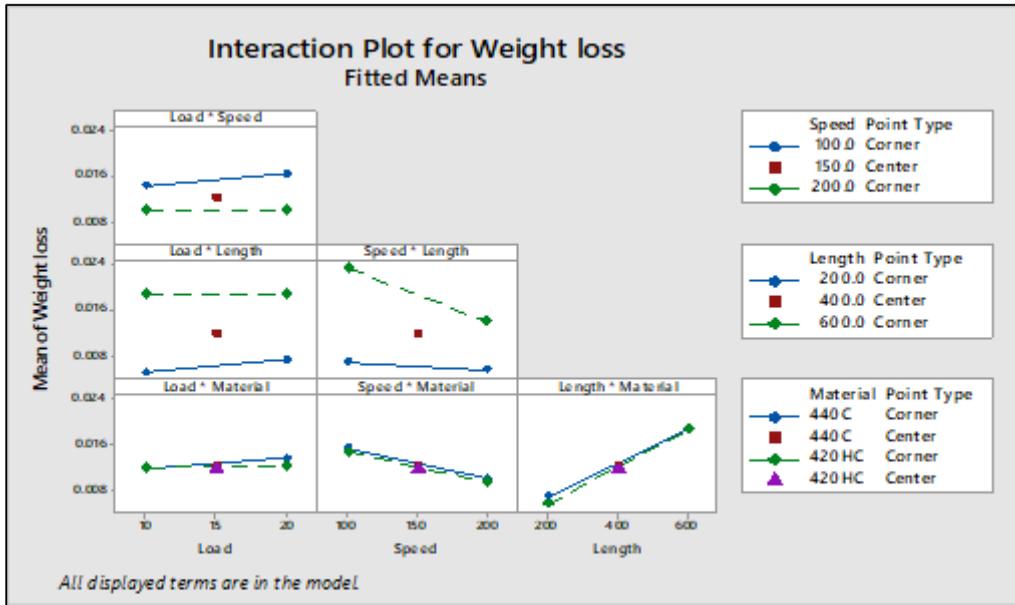
Figure 5: Interaction for weight loss

The Maim Effect Plots of Wear Parameters

The significance of the mass loss factors can be checked also by analyzing their main-effect-plots as illustrated in the following paragraphs:

Effect of Load on the Weight Loss

Figure 6 shows that the normal load factor has a negligible impact on the weight loss. As the applied load increases, the temperature of rubbing surface increases due to the frictional force. As the temperature increases, carbon atoms of Martensite steel diffuses out and formed carbides which leads to increase the material hardness. Therefore, the material resistance of weight loss increases due to the increment of material hardness which justify the small effect of load in the weight loss.
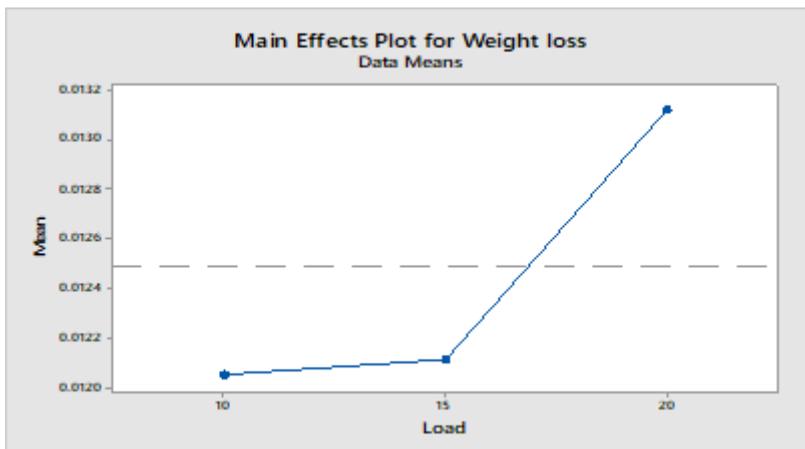
Figure 6: Main effect plot of the load factor

The hardness of the worn surfaces of AISI 440C and AISI 420 stainless steel subjected to 10N and 20N loads, 600 m sliding distance and 100 rpm sliding speed are included in table 3.

Table 3: material hardness at different loads

Material	Load (N)	Hardness (HRC)
AISI 440C	10	29
AISI 440C	20	53
AISI 420	10	
AISI 420	20	35

Sliding Speed Effect on the Weight Loss

The main effect of the speed plot is shown in Figure 7. It can be noted that the plot line is not horizontal which means the speed factor has effect in the weight loss. It can be noted also that the sliding speed has a negative effect on the weight loss.
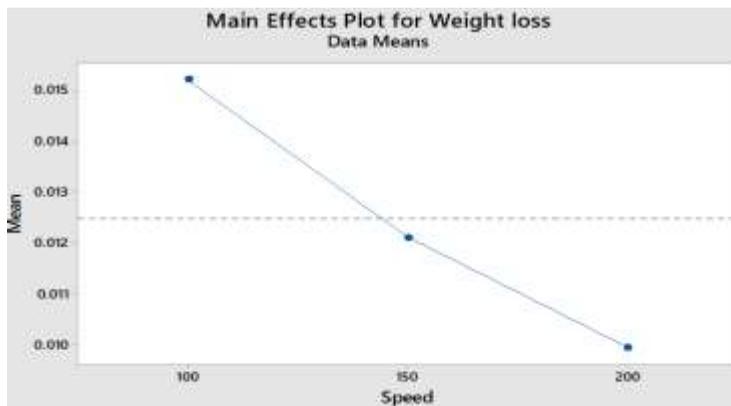
Figure 7: Main effect plot of the speed factor

Effect of Sliding Distance on the Weight Loss

The main effect plot of the length, shown in Figure 8, indicate that the length factor is significant because the line slop is not horizontal. It can be noticed from the plot that the length factor has a positive effect on the weight loss.
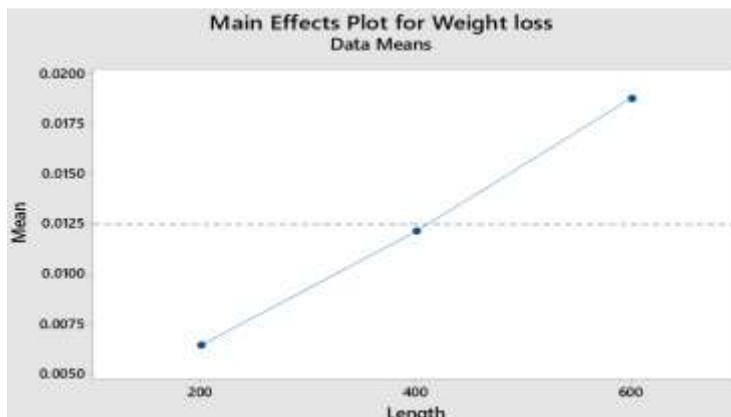
Figure 8: Main effect plot of the length factor

Effect of material on the weight loss

The main effect plot of the material, shown in Figure 9, indicate that the length factor is significant because the line slop is not horizontal. It can be noticed from the plot that the length factor has a positive effect on the weight loss.
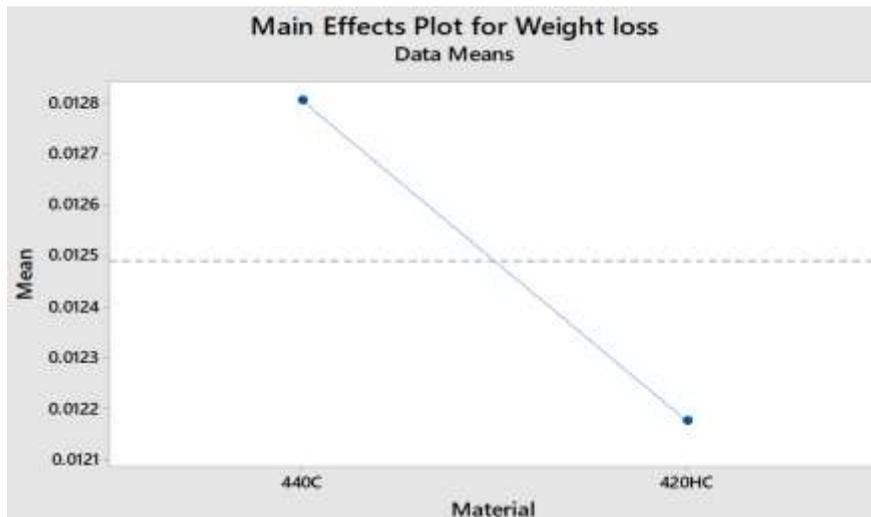
Figure 9: Main effect plot of the material factor

Model Adequacy Checking

The data of weight loss are examined by the residual plots as shown in Figures 10, 11, and 12. The normal probability plots in Figure 10 made a straight line referring to the normal distribution of the errors
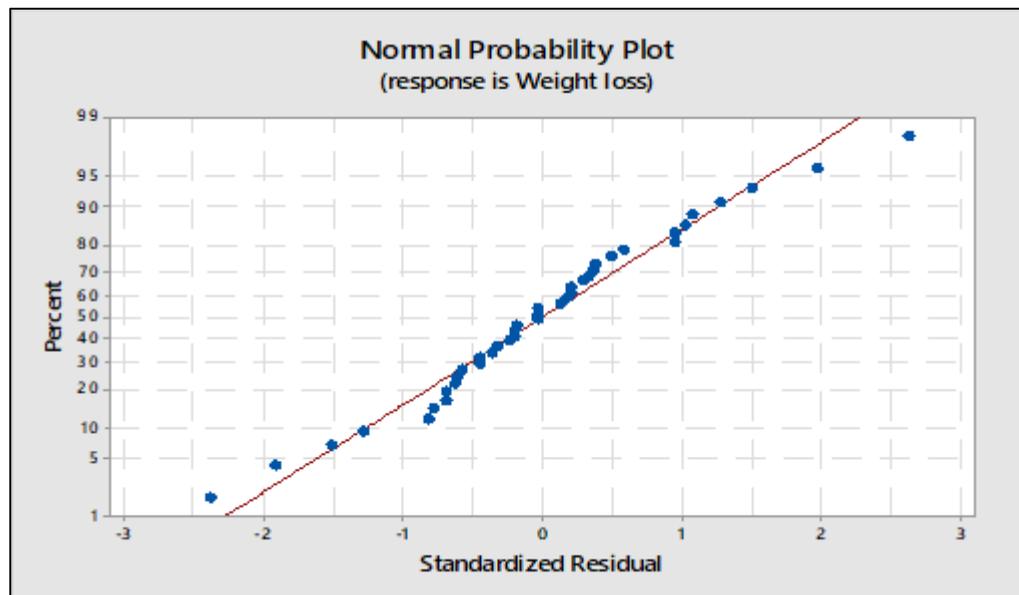
Figure 10: Standardized residual plot of the weight loss data

The plot of versus order in Figure 11 shows that the data are independent and they have not constant variability.
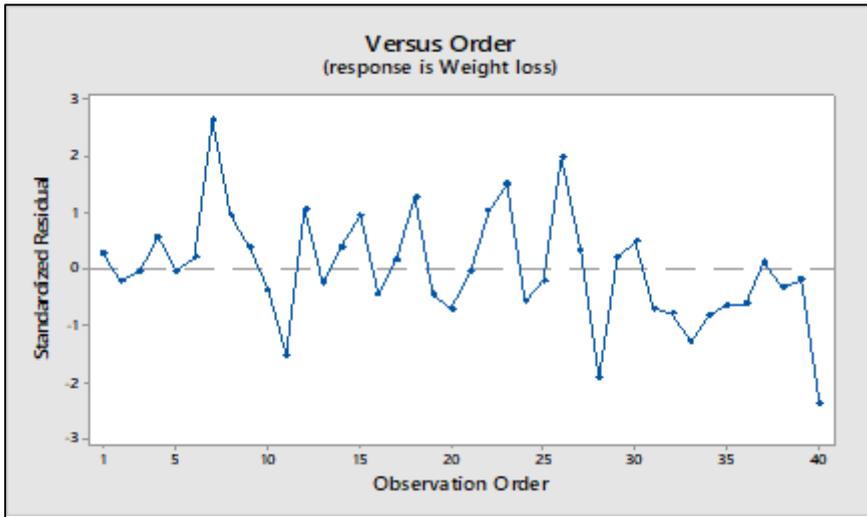
Figure 11: observation order of the standardized residual

The fitted value plot in Figure 12 show that the value of the response is randomly distributed.
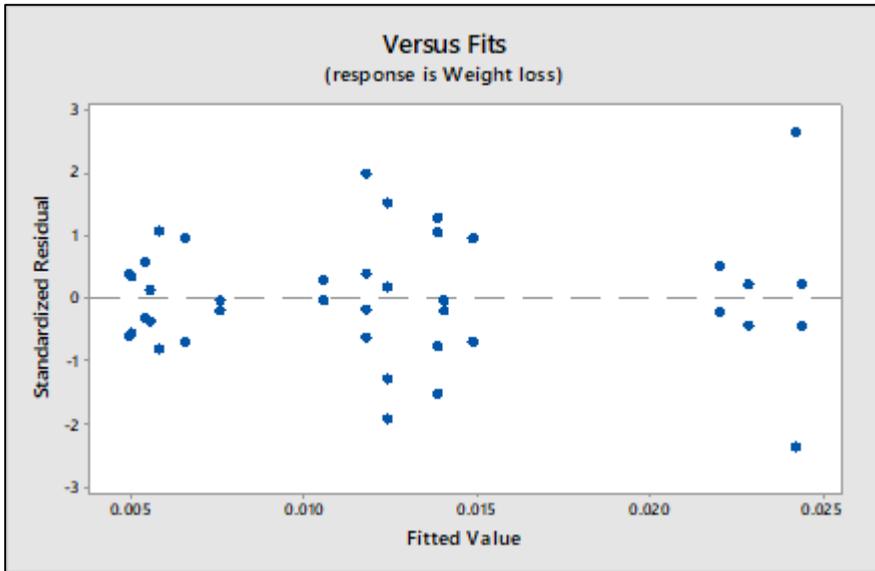
Figure 12: standardized residual of fitted value

Wear Rate Formula

The wear rate formula could include only the significant wear factors. The result of this paper shows that the sliding speed and the sliding distance are significant factors, but the normal load is not significant. Therefore, the formula 1 could be adjusted by removing the insignificant factor (normal load) and adding the significant factor (sliding speed).

To determine the relation between the sliding speed and the mass loss, several experiment are conducted by using a pin-on-disc machine at different sliding speeds with fixing the values of the normal load and sliding distance. By analyzing the experimental data, the obtained results demonstrate that the relation between the sliding speeds in addition to the mass loss can be represented by Michaelis–Menten equation as the following:

$$M = \frac{\theta 1 * S}{\theta 2 + S}$$

Where the mass loss (g) expressed by M, S: is the sliding speed (rpm), and θ1 and θ2: material dependent parameters

Then, the wear rate formula can be adjusted and expressed by the following equation:

$$W = \frac{M}{\rho L * \frac{\theta 1 * S}{\theta 2 + S}}$$

Where the wear rate (mm^3/m) is represented by W, and the mass loss (g) is represented by M, ρ: is the material density (g/mm3), L represents the length of the sliding distance (m), the sliding speed (rpm) expressed by S, as well as θ1 and θ2 are material dependent parameters

The estimation θ1 and θ2 parameters for AISI 440C are determined by Minitab. Table 4 includes the parameter estimation and the estimated standard error of the regression.

Fitted Line Plot
Mass Loss = 0.0265154 * 'Speed(rpm)' / (136.371 + 'Speed(rpm)')
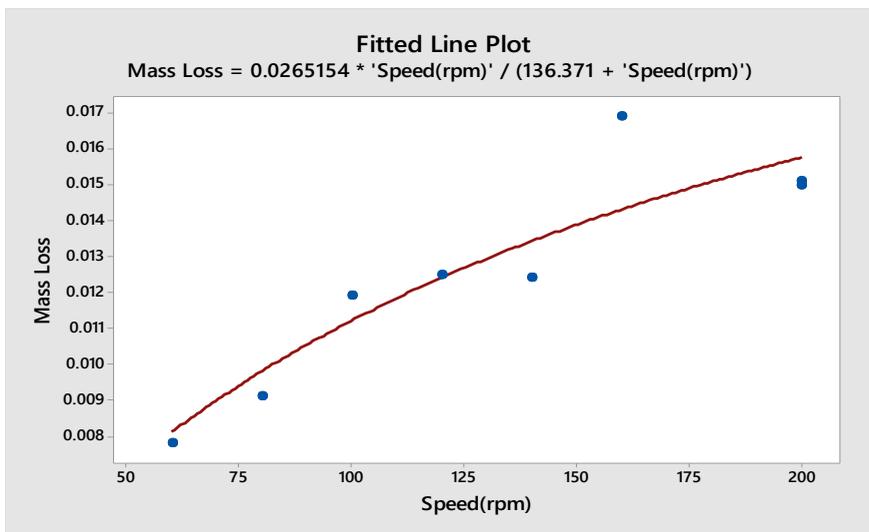
Figure 13: Fitted line of mass loss versus speed of AISI 440C steel

Table 4: Parameter Estimates of AISI 440C stainless steel

Parameter	Estimate	SE Estimate
Theta1	0.027	0.0054
Theta2	136.371	56.3862

The relation between the mass loss and the speed of AISI 440C are represented by the following equation:

Mass Loss 440 = 0.0265154 * 'Speed (rpm) ' / (136.371 + 'Speed (rpm) ')

Table 5: Lack of Fit

Source	DF	SS	MS	F	P
Error	6	0.0000098	0.0000016		
Lack of Fit	5	0.0000098	0.0000020	393.28	0.038
Pure Error	1	0.0000000	0.0000000		

S shows the average distance, which the observed values fall from the regression line. Thus, it is referring to how wrong the regression model is on average using the units of the response variable. Smaller values are better because it indicates that the observations are closer to the fitted line.

Examination of the Worn Surface Morphology

The morphology of the worn surface is examined for each material by using SEM images to investigate the wear mechanism. Figures 14, 15, and 16 show the worn surface of AISI 420 stainless steel sample after dry sliding wear test at 20 N normal load, 600 m sliding distance and 200 rpm sliding speed. The figures show that there are mixed wear mechanisms. For example, Figure 14 includes a delamination and abrasive wear mechanism, Figure 15 shows adhesion wear and Figure 16 shows an image includes the three types.
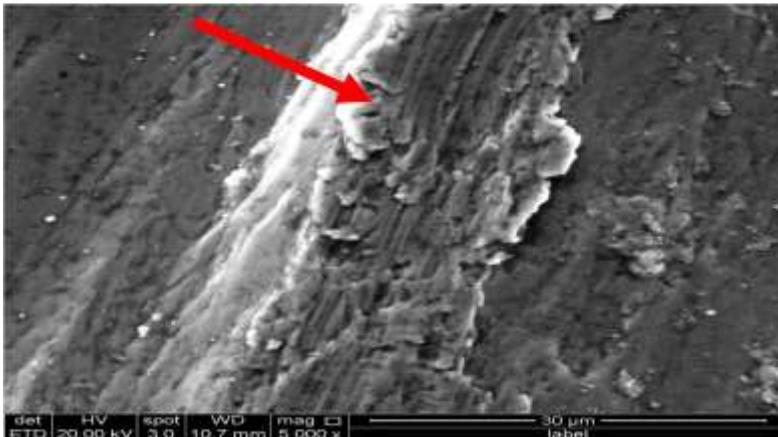
Figure 14: A delamination and abrasive wear mechanism
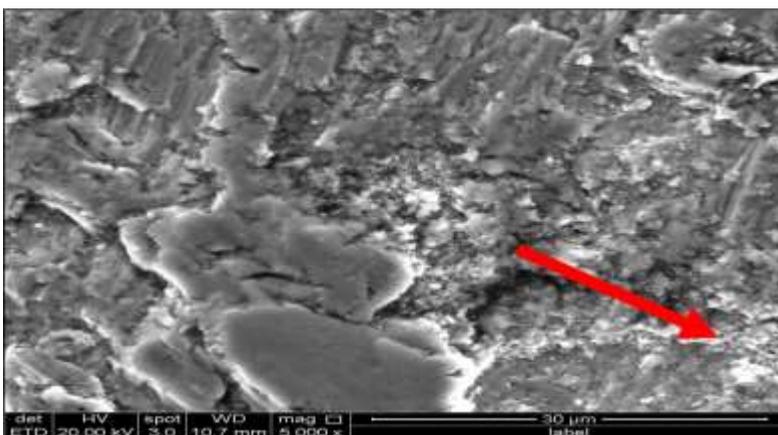
Figure 15: adhesion wear
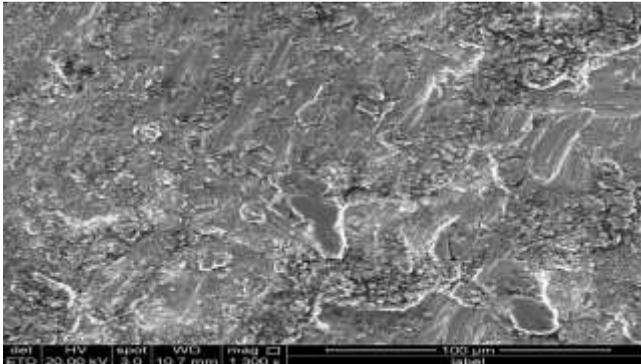
Figure 16: three types

Figures 17 and 18 show the worn surface of AISI 440C stainless steel sample after dry sliding wear test at 20 N normal load, 600 m sliding distance and 200 rpm sliding speed. Figure 17 includes an abrasive wear mechanism, and Figure 18 shows an image of abrasive, adhesion and delamination wear mechanisms.
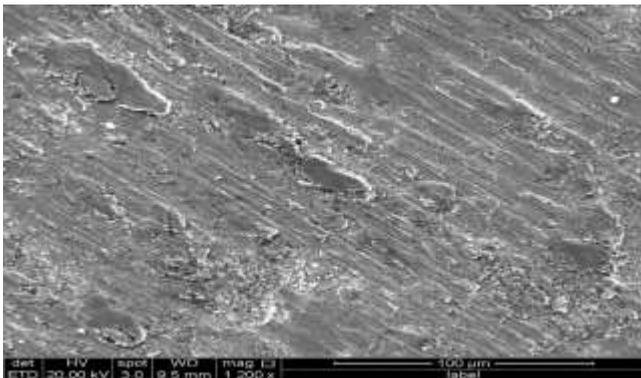
Figure 17: an abrasive wear mechanism
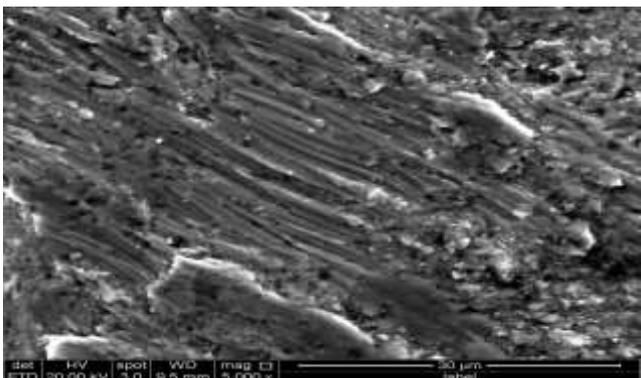
Figure 18: abrasive, adhesion and delamination wear mechanisms

Figures 19 and 20 show the worn surface of AISI 440C stainless steel sample after dry sliding wear test at 10 N normal load, 600 m sliding distance and 200 rpm sliding speed. Figure 19 shows an image abrasive, adhesion and delamination wear mechanisms, and Figure 20 includes an abrasive wear mechanism.
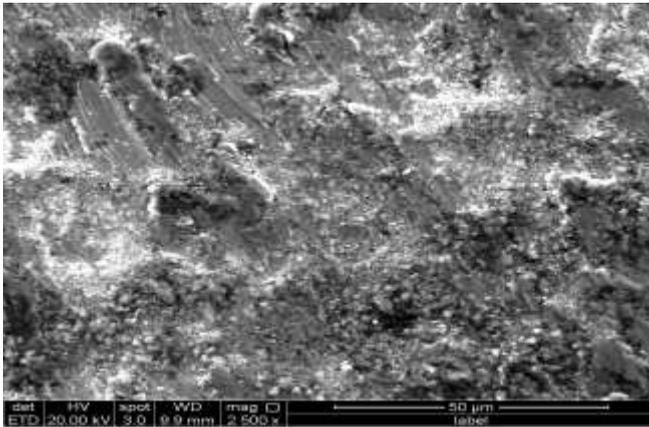
Figure 19: abrasive, adhesion and delamination wear mechanisms
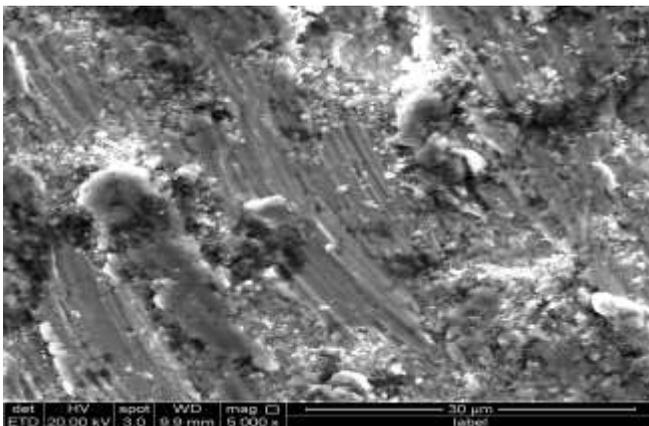
Figure 20: an abrasive wear mechanism
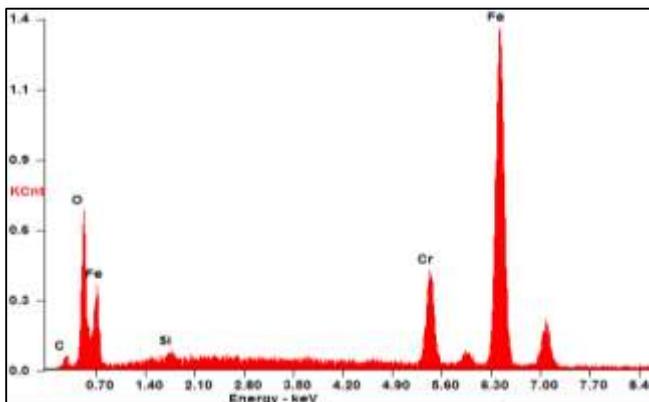
Figure 21: EDX image of AISI 440C stainless steel at 10N load, 100 rpm sliding speed and 600m sliding distance

Figures 21 and 22 include the EDX images of the worn surfaces at different loads. It can be observed from the EDX that the content of carbides in the worn surface at 20N load is higher than the carbides content at 10N load.
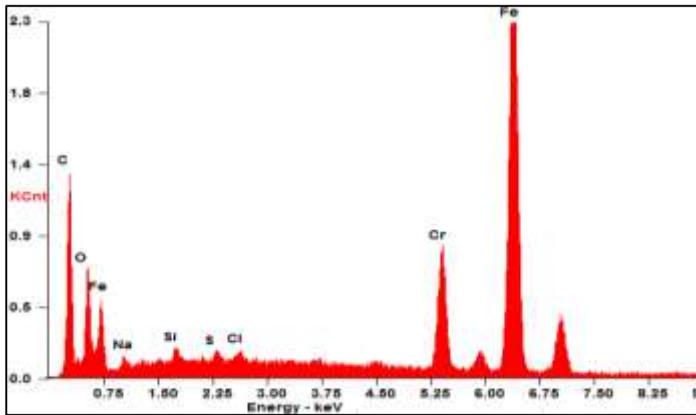
Figure 22: EDX image of AISI 440C stainless steel at 20N load, 100 rpm sliding speed and 600m sliding distance

CONCLUSION

The present research is accomplished to develop an empirical model to fit the true relationship between wear rate and the significant factors in the case of AISI 440C and AISI 420 materials. Four factors are studied in this research namely the applied load, the sliding distance, the sliding speed and the material using two replicate full factorial design. Throughout this research, an attempt was made to determine the most significant parameters that influence the wear performance. The results showed that the sliding distance is the most significant factor influencing the mass loss with 72.28% contribution followed by sliding speed (13.32%contribution). Further, the applied load and material have a negligible effect on the mass loss. A relation between sliding speed and the mass loss was determined. Moreover, a relation between the wear rate and the significant factors are developed. The list of the following points includes the conclusions drawn from this research:

- The applied load and material have a negligible effect on the mass loss.
- The sliding speed and the sliding distance have a significant effect on the mass loss.
- Increasing the sliding distance leads to increase of the mass loss and the increasing of the sliding speed leads to reduce the mass loss.

REFERENCES

Andersson J. (2012) Modelling of wear and tribofilm growth, Luleå tekniska universitet.

Andersson J., Almqvist A., and Larsson R. (2011) Numerical simulation of a wear experiment. In: Wear 271.

Berglund K. and Shi Y. (2017) Friction and Wear of Self-Lubricating Materials for Hydropower Applications under Different Lubricating Conditions, In: Lubricants 5.3.

Blau P. J. (2015) How common is the steady-state? The implications of wear transitions for materials selection and design, In: Wear 332.

Boher C. (2009) A wear model based on cumulative cyclic plastic straining, In: Wear 267.

Cavalieri F. J., Zenklusen F., and Cardona A., (2016) Determination of wear in internal combustion engine valves using the finite element method and experimental tests. In: Mechanism and machine theory 104.

Chongyi Ch., Chengguo W., and Ying J. (2013) Study on numerical method to predict wheel/rail profile evolution due to wear, In: Wear 269.

Wang Y., Stephen M., and Hsu (1996) The effects of operating parameters and environment on the wear and wear transition of alumina, Wear 195.

--0--